81% Conversion efficiency in frequency-stable continuous-wave parametric oscillation

G. Breitenbach, S. Schiller, and J. Mlynek

Fakultät für Physik, Universität Konstanz, D-78434 Konstanz, Germany

Received April 10, 1995; revised manuscript August 2, 1995

We have studied doubly resonant parametric oscillation in the regime of maximum conversion efficiency. A monolithic $MgO:LiNbO_3$ resonator with a threshold of 28 mW, pumped by a frequency-doubled Nd:YAG laser, was employed. With an active frequency-stabilization scheme, single-mode operation without mode hops at 105 mW combined signal and idler output power was achieved at a pump power four times above threshold, with a conversion efficiency of 81%. Excellent agreement between theory and experiment was found for the dependence of efficiency and depletion on pump power. The efficiency and the nearly complete pump depletion of 94% were limited only by imperfect mode matching of the pump wave and by the small cavity losses. © 1995 Optical Society of America

1. INTRODUCTION

A primary goal in the development of cw resonant nonlinear optical devices is the achievement of high conversion efficiency and frequency-stable operation. Recently, conversion efficiencies greater than 80% have been demonstrated for cw second-harmonic generation (SHG) of infrared lasers at the 0.1–1-W power range.[1,2] In the reverse process of cw downconversion the highest efficiency reported was at the 40% level.[3]

In a historic paper, Siegman[4] showed that the maximum conversion efficiency of a doubly resonant optical parametric oscillator (DRO) that employs a standing-wave cavity and a unidirectional, nonresonant pump wave is limited to 50%. This limit, reached when the pump power is four times above threshold, occurs because of back conversion of the backward-propagating signal or idler waves to the pump frequency by the sum-frequency-generation (SFG) process. It is well known that one can circumvent the 50% limit by reflecting the pump beam back through the crystal or by using a ring cavity.[5] With such an arrangement 100% conversion efficiency is theoretically possible. In this paper we report an experimental investigation of the high-pump-depletion/high-conversion-efficiency of the operating regime of cw DRO's by employing the double-pass geometry for the pump beam.

The implementation of schemes for continuous tuning of the output frequencies of cw DRO's and for obtaining a high degree of stability of the output frequencies has recently become a focus of DRO development. High frequency stability is possible only if a stable reference is employed. This can be the pump frequency itself, generated by an actively frequency-stabilized or intrinsically stable laser source, or it can be realized by a stable cavity geometry. A continuous tuning system will have to achieve highly accurate control of three tuning parameters, at least one of which will require active feedback control by means of an error signal derived from the detunings of the signal and the idler frequencies relative to the cavity-mode frequencies. Usually this parameter is the cavity optical path length. We demonstrate here that, for a monolithic DRO, it is possible to use the pump frequency as a feedback parameter instead because the cavity length is intrinsically stable. The pump source that we have developed for this purpose has a 20-GHz continuous tuning range at 532 nm, which is in principle suited for DRO output tuning over 10 GHz.

This paper is structured as follows. We discuss basic issues of the theory of DRO's, such as threshold, conversion efficiency, depletion, and frequency tuning, in Section 2. Experimental results are given in Section 3.

2. THEORY

A. DRO Conversion Efficiency and Pump Depletion

The theory of the conversion efficiency of a DRO as a function of pump power was given by Bjorkholm[5] for the case of plane pump, signal, and idler waves. As the effect on the pump depletion of DRO's employing a focused pump beam and focused resonator modes was unclear,[6] we use here a general theory that is also applicable to focused waves. Its derivation will be given elsewhere.[7]

We consider a nearly degenerate type-I DRO whose signal and idler frequencies (ω_s, ω_i, respectively) are sufficiently close that their intracavity loss and output couplings as well as their waists are nearly equal. The crucial assumption is that the signal and the idler waves are TEM_{00} modes and that the nonresonant pump wave (frequency ω_p) is a TEM_{00} mode with one half the beam area. This assumption ensures optimum spatial overlap and therefore a limiting efficiency of 100%. The equations of motion for the intracavity signal ($\overline{\alpha}_s$) and idler ($\overline{\alpha}_i$) fields are then given, in the notation customary in quantum optics, by

$$\dot{\overline{\alpha}}_{i/s} = -(\gamma + i\Delta_{i/s})\overline{\alpha}_{i/s} + \sqrt{\nu}K^*\alpha_{p,\mathrm{in}}\overline{\alpha}_{s/i}{}^* - \nu D|\overline{\alpha}_{s/i}|^2\overline{\alpha}_{i/s}\,. \quad (1)$$

Here the intracavity fields are defined in terms of their slowly varying electric-field envelopes $E_{i/s}$ by $\overline{\alpha}_{i/s} = (\tau n_{i/s}/\omega_{i/s})^{1/2}E_{i/s}$, where τ is the round-trip time of the

0740-3224/95/112095-07$06.00

cavity, n is the refractive index, and ω is the angular frequency. The pump field incident upon the nonlinear medium and its envelope are related by $\alpha_{p,\mathrm{in}} = i(n_p/\omega_p)^{1/2}E_{p,\mathrm{in}}$. We assume below that $\omega_s \simeq \omega_i \simeq \omega_p/2$, $n_s \simeq n_i \simeq n_p$.

The first term on the right-hand side in Eq. (1) describes the decay of the intracavity fields due to outcoupling (mirror power transmission T) and internal loss (power loss fraction A per round trip), where $\gamma = (T + A)/2\tau$ is the total decay rate of the amplitudes. $\Delta_{s/i}$ are the detunings of the signal and the idler waves from cavity resonance frequencies. The second term is the parametric coupling between the signal or the idler wave and the pump wave. The last term describes upconversion of the circulating signal and idler waves to the pump wave. The nonlinear coefficient $\sqrt{\nu} = |\kappa|L_m/2\tau$, where κ is proportional to the d_{eff} coefficient[8] and L_m is the propagation distance through the nonlinear medium per roundtrip. The phase-matching coefficients D, K are complex, dimensionless numbers that depend on the wave-vector (phase) mismatch $\Delta k = k_p - k_s - k_i$, on the focusing, and on additional phase shifts between the signal or the idler wave and the pump wave that may occur on a round trip, e.g., on reflection at a mirror.[2,5,9,10]

To calculate depletion and conversion efficiency, we require expressions that relate the fields leaving the cavity, $\alpha_{p,\mathrm{out}}$ and $\alpha_{i/s,\mathrm{out}}$, to the incident ones:

$$\alpha_{p,\mathrm{out}} = \alpha_{p,\mathrm{in}} - 2\sqrt{\nu}\,K\overline{\alpha}_i\overline{\alpha}_s\,, \tag{2}$$

$$\alpha_{i/s,\mathrm{out}} = \sqrt{2\gamma_c}\,\overline{\alpha}_{i/s}\,. \tag{3}$$

Here $\gamma_c = T/2\tau$ is the relaxation rate due to outcoupling alone, and the external signal and idler fields are defined as $\alpha_{i/s,\mathrm{out}} = (n_{i/s}/\omega_{i/s})^{1/2}E_{i/s,\mathrm{out}}$. The beam powers leaving and entering the resonator are given by

$$P_{i/s/p,\mathrm{in/out}} = \frac{\pi}{4}\sqrt{\frac{\epsilon_0}{\mu_0}}\,\omega_{i/s/p}w_{i/s/p}{}^2|\alpha_{i/s/p,\mathrm{in/out}}|^2, \tag{4}$$

where w are the respective waists at the foci inside the cavity. For signal and idler waves, $w_i \simeq w_s$ are the waists of the resonator TEM_{00} mode. The assumption of optimum focusing stated above implies that the pump-beam waist $w_p{}^2 = w_{i/s}{}^2/2$.

Equations (1)–(3) are valid for a high-finesse cavity, that is, in the limit $T, A \ll 1$. Special cases of Eqs. (1)–(3) for near-field focusing and $\Delta k = 0$ were derived and discussed in Refs. 11–14. For concreteness, we give the explicit forms of the phase-matching coefficients in the near-field case[15]:

$$K_{\mathrm{NF}} = \mathrm{sinc}(\Delta k L_m/2),$$
$$D_{\mathrm{NF}} = -\frac{2i}{\Delta k L_m}[1 - \exp(-i\Delta k L_m/2)\mathrm{sinc}(\Delta k L_m/2)]. \tag{5}$$

In the following calculations we require only a very general relationship between K and D.[7] Energy conservation for the DRO is expressed by the power balance (with $\omega_s \simeq \omega_i \simeq \omega_p/2$):

$$|\alpha_{p,\mathrm{in}}|^2 = |\alpha_{p,\mathrm{out}}|^2 - |\alpha_{i,\mathrm{out}}|^2 + |\alpha_{s,\mathrm{out}}|^2 + 2(\gamma - \gamma_c)(|\overline{\alpha}_i|^2 + |\overline{\alpha}_s|^2) + \mathrm{d}(|\overline{\alpha}_i|^2 + |\overline{\alpha}_s|^2)/\mathrm{d}t\,, \tag{6}$$

from which one obtains, using Eqs. (1)–(3):

$$\mathrm{Re}\,D = |K|^2. \tag{7}$$

In general, the imaginary part of D is nonvanishing. In the near-field case, Eqs. (5) show that this part vanishes only for perfect phase match, $\Delta k = 0$. There is thus, in general, a nonlinear contribution to the detuning of signal and idler waves in Eq. (1), and this contribution is given by

$$\Delta_{i/s}{}^{\mathrm{NL}} = \nu|\overline{\alpha}_{s/i}|^2\,\mathrm{Im}\,D\,. \tag{8}$$

This detuning can be interpreted as an effective Kerr cross coupling due to cascading.[15]

Conversion efficiency and depletion are defined by

$$\eta = \frac{P_{i,\mathrm{out}} + P_{s,\mathrm{out}}}{P_{p,\mathrm{in}}}, \qquad d = \frac{P_{p,\mathrm{out}}}{P_{p,\mathrm{in}}}\,. \tag{9}$$

We evaluate these expressions for the stationary state ($\dot{\overline{\alpha}}_{i/s} = 0$), taking the input pump field $\alpha_{p,\mathrm{in}}$ as real and positive for simplicity. For given detunings $\Delta_{i/s}$ and phase-matching coefficients K, D, the intracavity signal and idler powers are determined by two fourth-order equations. Accordingly, the conversion efficiency and depletion will also, in general, depend on the detunings. As the detunings are, in principle, arbitrary, we consider those detunings that yield the maximum conversion efficiency. To this end $|\overline{\alpha}_{s/i}|^2$ are maximized with respect to Δ_i and Δ_s. The optimum detunings are found to be given by

$$\Delta_{i/s}{}^{\mathrm{opt}} = -\nu|\overline{\alpha}_{s/i}{}^{\mathrm{max}}|^2\,\mathrm{Im}\,D\,. \tag{10}$$

By comparison with Eq. (8) we can see that for optimum efficiency the cavity detunings must be such that they just compensate the detuning caused by the nonlinear round-trip phase shift. For perfect phase matching, when $\mathrm{Im}\,D = 0$, we recover the well-known result that the efficiency is maximum for zero detuning. The intracavity fields corresponding to the above detunings are given by

$$|\overline{\alpha}_s^{\mathrm{max}}|^2 = |\overline{\alpha}_i^{\mathrm{max}}|^2 = \frac{\sqrt{\nu}\,|K|\alpha_{p,\mathrm{in}} - \gamma}{\nu\,\mathrm{Re}\,D}\,. \tag{11}$$

Inserting Eq. (11) into Eqs. (9) and making use of Eqs. (2), (3), and (7), we obtain

$$\eta = \frac{4T}{A+T}\left(\sqrt{\frac{P_{\mathrm{th}}}{P_{p,\mathrm{in}}}} - \frac{P_{\mathrm{th}}}{P_{p,\mathrm{in}}}\right), \tag{12}$$

$$d = \left(2\sqrt{\frac{P_{\mathrm{th}}}{P_{p,\mathrm{in}}}} - 1\right)^2, \tag{13}$$

with

$$P_{\mathrm{th}} = \frac{\pi}{4}\sqrt{\frac{\epsilon_0}{\mu_0}}\,\omega_p w_p{}^2\,\frac{\gamma^2}{\nu|K|^2} \tag{14}$$

being the threshold corresponding to zero detuning, that is, the minimum threshold. Expressions (12) and (13) constitute the important result that the functional forms of maximum conversion efficiency and corresponding de-

pletion of a high-finesse DRO at a given pump power P are independent of focusing and wave-vector mismatch. This result represents a generalization of the result obtained by Bjorkholm.[5] Focusing and wave-vector mismatch do determine the value of the DRO threshold power, however. The highest conversion efficiency, $\eta_{\max} = T/(A + T)$, and complete depletion, $d = 0$, are reached at four times above threshold, $P_{p,\text{in}} = 4P_{\text{th}}$.

To relate this result to a measurable nonlinear coefficient, we consider the inverse process of SFG. Equation (2) shows that, in the absence of an incident pump wave ($\alpha_{p,\text{in}} = 0$), signal and idler powers $P_{i,\text{circ}}$, $P_{s,\text{circ}}$ circulating in the cavity generate a sum-frequency wave of power P_2 with an efficiency of

$$\Gamma_{\text{SFG}} = \frac{P_2}{P_{i,\text{circ}} P_{s,\text{circ}}} = \frac{16}{\pi} \sqrt{\frac{\mu_0}{\epsilon_0}} \frac{\tau^2}{\omega_p {w_p}^2} \nu |K|^2. \tag{15}$$

In the near-degeneracy case assumed here, Γ_{SFG} is equal to $4\Gamma_{\text{SHG}}$, where Γ_{SHG} (in W^{-1}) is the nonlinear coefficient for SHG. Combining Eqs. (14) and (15), we finally obtain the well-known expression

$$P_{\text{th}} = \frac{(T + A)^2}{4\Gamma_{\text{SHG}}}, \tag{16}$$

with

$$\Gamma_{\text{SHG}} = \frac{\mu_0 n \kappa^2}{\pi} L_m\left(\frac{L_m}{2z_r} |K|^2\right), \tag{17}$$

with n being the refractive index and z_r denoting the Rayleigh range. The factor given in parentheses is the focusing factor. For a simple cavity in which no relative mirror phase shifts between signal or idler and pump occur, the focusing factor is equal to the Boyd–Kleinman focusing factor h.[16] The explicit form for the focusing factor of the resonator used here, which takes into account an arbitrary mirror phase shift, was discussed in Ref. 2.

In closing this section, we emphasize again that expressions (12)–(16) hold for the case of maximum conversion, i.e., for zero total (linear + nonlinear) detunings.

B. Tuning of DRO Frequencies

Continuous tuning can be achieved in a controlled fashion through the use of three tuning parameters that are varied so as to satisfy the resonance conditions for signal and idler frequencies and to obtain optimum wave-vector mismatch.[17] The tuning parameter that most directly controls the wave-vector mismatch is the crystal temperature (or angular orientation). The remaining tuning parameters depend on the DRO type. For a single-cavity DRO, cavity length and pump frequency can be used. When a monolithic DRO is employed, the cavity-length parameter is accessible through an electric field causing an electro-optic and/or piezoelectric optical path length change.[17] For type-I interaction, initial research on DRO tuning was performed by Nabors *et al.*[6] Below we summarize the basic features of type-I DRO tuning and frequency control.[17]

The range (but not the precise values) of the DRO output wavelengths are governed by the requirement of high parametric gain or, equivalently, small wave-vector mismatch Δk. Near degeneracy, Δk can be Taylor expanded as

$$\Delta k(\nu_p, \nu_s, T) = \frac{\partial \Delta k}{\partial \nu_p} \Delta \nu_p + \frac{1}{2} \frac{\partial^2 \Delta k}{\partial {\nu_s}^2} \Delta {\nu_s}^2 + \frac{\partial \Delta k}{\partial T} \Delta T. \tag{18}$$

The expansion is given in terms of deviations of the pump frequency $\Delta\nu_p = \nu_p - 2\nu_0$, the temperature $\Delta T = T - T_0$, and the signal frequency $\Delta\nu_s = \nu_s - \nu_0$ from their values at degeneracy. The partial derivatives are all taken at the degeneracy temperature T_0 and at the degeneracy frequencies ν_0 and $2\nu_0$. The numerical expression for MgO:LiNbO_3 pumped by $\lambda_0/2 = 532$ nm is[17]

$$\Delta k = [3.4\Delta\nu_p/\text{GHz} - 8.7 \times 10^5 (\Delta\nu_s/\nu_0)^2 + 749\Delta T/\text{K}]\text{m}^{-1}. \tag{19}$$

This expression is complemented by the description of the behavior of the actual values of the output frequencies when the remaining parameters of the DRO undergo changes. In this study we consider the case in which the cavity length and the temperature are independent tuning parameters and the pump frequency is regulated by electronic feedback control. The regulation criterion is the fulfillment of the cluster equation, the sum of the signal and idler cavity resonance equations.

The characteristics of this type of lock can be cast in quantitative form. Consider a DRO whose monolithic cavity (round-trip length L) is subject to small changes in round-trip length (δL) and temperature (δT) due to external control or environmental perturbations. The cavity resonance frequencies change by the amounts $\delta\nu_s^{(c)}$, $\delta\nu_i^{(c)}$ in response. The pump frequency is actively controlled such that the average detuning of signal and idler frequencies from cavity-mode frequencies does not change, $\delta\nu_s - \delta\nu_s^{(c)} + \delta\nu_i - \delta\nu_i^{(c)} = 0$. By expanding the cluster equation and the signal resonance condition in Taylor series near the degeneracy point T_0, ν_0, it is easy to derive cause–effect relationships between the required pump frequency adjustment $\delta\nu_p$ and the induced signal cavity frequency change $\delta\nu_s$ caused by the assumed length and temperature changes.[18] These relationships are given by

$$\frac{\delta\nu_s^{(c)}}{\nu_s} = -\frac{1}{2}\left(\frac{\delta L}{L} + A\delta T\right)(B + C\Delta\nu_s)^{-1},$$
$$\frac{\delta\nu_p}{2\nu_0} = -\frac{1}{2}\left(\frac{\delta L}{L} + A\delta T\right)B(B^2 - C^2{\Delta\nu_s}^2)^{-1}. \tag{20}$$

The coefficients are given by

$$A = \left[\frac{1}{n_1}\frac{\mathrm{d}n_1(\nu_0, T)}{\mathrm{d}T} + \alpha_T\right], \tag{21}$$

$$B = \frac{1}{2}\left[\frac{\nu_0}{n_1}\frac{\mathrm{d}n_1(\nu_s, T_0)}{\mathrm{d}\nu_s} + 1\right], \tag{22}$$

$$C = \frac{1}{n_1}\left[\frac{\mathrm{d}n_1(\nu_s, T_0)}{\mathrm{d}\nu_s} + \frac{\nu_0}{2}\frac{\mathrm{d}^2 n_1(\nu_s, T_0)}{\mathrm{d}{\nu_s}^2}\right]. \tag{23}$$

and are evaluated at the degeneracy point. Here n_1 is the refractive index of the signal wave and α_T is the coefficient of thermal expansion.

Under the assumption that the detuning of signal and idler waves relative to cavity resonance frequencies does not change, the cavity shift $\delta\nu_s^{(c)}$ is equal to the oscillation frequency shift $\delta\nu_s$. Expressions (20) are then an example of a three-parameter tuning relation discussed by Eckardt *et al.*[17] Here the three tuning parameters are cavity length L, temperature T, and pump frequency ν_p, with the last being a slave parameter.

Equations (20) can be simplified near degeneracy, where the $C\Delta\nu_s$ term is negligible (for MgO:$LiNbO_3$, $C = 1.2 \times 10^{-16}$ s). One then finds that the correction to be applied to the pump frequency is twice as large as the tuning of the signal and the idler frequencies:

$$\delta\nu_{s/i} = \delta\nu_p/2 = -[2.7 \times 10^5(\delta L/L) + 5.3\delta T/\mathrm{K}]\mathrm{GHz}. \tag{24}$$

Expressions (19) and (24) are useful guides to the coarse- and fine-tuning behavior of a type-I DRO. In Section 3 they are applied to give estimates of the locking range of the laser and the output wavelength tuning range.

3. EXPERIMENT

A. Nonlinear Resonator

To study parametric oscillation in the high-conversion regime, we chose a cavity design that not only permits a large ratio T/A and preserves an accessible threshold level. We used a low-loss monolithic resonator[6,19,20] whose good mechanical stability and large cavity linewidth considerably simplify frequency-stable operation. The resonator is of the standing-wave type and was previously described in Ref. 2. It is fabricated from 5% MgO-doped $LiNbO_3$ and has a length of 7.5 mm. The crystal c axis is perpendicular to the length. Gold electrodes were evaporated onto the crystal sides perpendicular to the c axis for modulation purposes.

The end faces of the crystal are spherically polished to have 10-mm radii of curvature, yielding mode waists $w = 27\ \mu$m for a wavelength of 1064 nm. Dielectric mirrors were deposited on the end faces. One is the output coupler, with nominal $T = 2.1\%$ transmission at 1064 nm and near-complete transmission at 532 nm. The back reflector is highly reflecting for the signal and the idler waves as well as for the pump wave, so that they interact over the full round-trip distance of 15 mm. The relative reflection phase shift between the signal or the idler wave and the pump wave at the back reflector is unknown. Irrespective of the actual value of this phase shift, the DRO will oscillate at signal and idler wavelengths such that the corresponding wave-vector mismatch Δk yields a large squared nonlinear coefficient $|K|^2$. Estimates[2,10] indicate that even the worst-case mirror phase shift yields a squared nonlinear coefficient not less than a factor of 2 smaller than the maximum possible value for optimum mirror phase shift.

A necessary condition for achieving high conversion efficiency is a correspondingly high escape efficiency $T/(A + T)$. The sum $T + A$ of mirror transmission and internal loss can easily be determined from the measured finesse $\mathcal{F} = 265$ as $T + A = 2.4\%$. To verify that the escape efficiency is high, the results of SHG from 1064 to 532 nm can be used. Indeed, the theoretical maximum conversion efficiency for externally resonant SHG is $T/(A + T)$,[13] identical to that of a DRO. For the present device, Paschotta *et al.*[2] obtained 82% conversion efficiency at a 1064-nm input power of 120 mW. As the fraction of input power coupled into the cavity was 94%, we can infer a corrected conversion and thus a cavity escape efficiency of 88%. This result implies a round-trip cavity loss $A = (0.3 \pm 0.1)\%$. The nonlinear coefficient was measured to be $\Gamma_{\mathrm{SHG}} = 0.48\%/\mathrm{W}$ at the optimum crystal temperature.

B. Experimental Setup

A schematic of the experimental setup is shown in Fig. 1. As a pump source for the DRO, a single-frequency, diode-laser-pumped Nd:YAG ring laser with 500-mW output power (Lightwave Electronics Model 122) is used. A harmonic wave at 532 nm is generated by resonant SHG in a standing-wave MgO:$LiNbO_3$ resonator. The doubler cavity consists of a 7.5-mm-long crystal with one flat face and one $R_1 = 10$ mm spherical face and an $R_2 = 25$ mm input coupler mirror [antireflection coated (532 nm), T(1064 nm) = 3.5%] mounted on a piezoelectric actuator. The back coating of the crystal is highly reflecting for both 1064 and 532 nm. A frequency-locking circuit is used to lock the cavity to the laser frequency. A modified technique[21] is employed, with electro-optic modulation of the crystal itself. When optimized, the frequency doubler generates a 532-nm pump wave with as much as 200-mW power at 70% conversion efficiency and power fluctuations of less than 0.2%. Typically, the doubler is operated with nonoptimal mode match of the input wave, emitting 150 mW at 532 nm with 300-mW input power at 1064 nm. By tuning the laser frequency, the harmonic frequency is continuously and rapidly tunable over 20 GHz.

Before being injected into the DRO, the pump wave passes through an optical isolator that prevents back

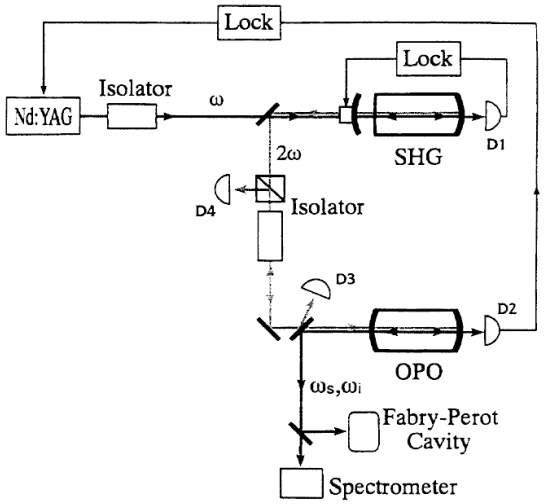

Fig. 1. Schematic of the experimental setup. The SHG and the optical parametric oscillator (OPO) $LiNbO_3$ crystals are both temperature stabilized at the phase-matching temperature (near 110 °C). For simplicity, the circuits for electro-optic modulation of the crystal resonators used for the frequency stabilization of the OPO output and of the doubler cavity length are omitted. D1–D4 are photodetectors.

reflection into the doubling cavity. The output wavelengths of the DRO are analyzed by a grating spectrometer, and a scanning Fabry–Perot cavity allows us to verify single-mode oscillation.

C. Measurement of the Input–Output Behavior

A good overlap between the pump wave and the resonator mode is crucial for obtaining a high conversion efficiency. To optimize the performance of the DRO, we generated 0.1-ms-duration pump pulses by scanning the doubler cavity length. When the pump pulses reach a certain power, the DRO starts to oscillate and emits signal and idler pulses, and the power of the reflected pump pulse declines. The pump-wave focusing and alignment were optimized to produce maximum pump depletion.

By operating the DRO in the long-pulse mode (where the pulse length is much longer than the oscillation buildup time), we can obtain the full dependence of efficiency and depletion on input pump power and perform an accurate comparison with Eqs. (12) and (13). Figure 2 shows the time traces of an input pump pulse, the reflected pump pulse, and the infrared output pulse. From such traces the input–output behavior of the DRO can easily be obtained. Figure 3(a) shows the depletion of the pump and the generated infrared power as a function of input power. The measured threshold of 28 mW agrees well with the expected value [Eq. (16)]. As shown in Fig. 3(b), a pump depletion of 95% was achieved at a pump level four times above threshold. The conversion efficiency from pump to combined signal and idler power reached a maximum of (84 ± 5)%. The theoretical fits shown in Figs. 3(a) and 3(b) are obtained from expressions (12) and (13), modified to account for imperfect pump-wave mode match. Denoting by $P_{p,\mathrm{in}} = (1 - \epsilon)P_{p,\mathrm{in}}^{\mathrm{tot}}$ the fraction of pump power actually available to pump the infrared modes, the fit yields $\epsilon = 5\%$, which indicates a mode overlap of 95% between the pump mode and the resonator mode. When corrected for finite ϵ, the maximum conversion efficiency for parametric generation coincides with that for resonant SHG[2] within the experimental error.

D. Frequency Stabilization and Tuning

DRO frequency-stabilization techniques usually use the pump frequency as a reference and actively stabilize the DRO cavity length to suppress mode and cluster hops.[3,6,22,23] If the DRO is of the monolithic type, the opposite procedure can be employed. Because the modes of a monolithic resonator thermally stabilized at the millikelvin level can provide frequency references with a stability at the 10-MHz level, one can also obtain stable output frequencies by slaving the pump frequency to the DRO. The present locking scheme is based on controlling the pump frequency such that the cluster frequency condition is satisfied. Its implementation is depicted in Fig. 1. The error signal to be fed back to the pump laser frequency actuator is generated in a way that is analogous to the doubler cavity lock: the DRO crystal is electro-optically modulated at 18 MHz (the resonator FWHM linewidth being 34 MHz) with a 0.1-V peak-to-peak signal. The corresponding optical path length modulation leads to amplitude modulation of the signal and the idler waves if their detuning is nonzero. The modulation is detected on the infrared waves transmitted through the highly reflecting side of the resonator. Although the signal and the idler waves each generate a respective error signal, the single detector employed does not discriminate between the two; instead the photocurrents caused by the two error signals are added, which results in a sum error signal that gives the average devi-

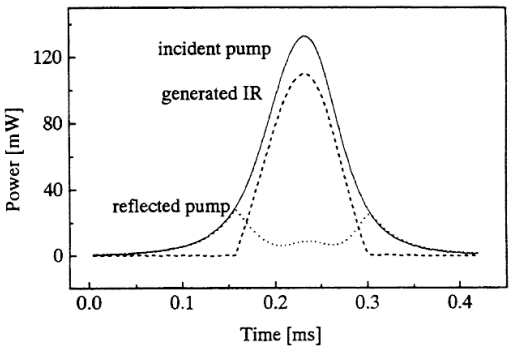

Fig. 2. High-efficiency parametric generation in pulsed operation. Solid curve, input 532-nm pump pulse incident upon the DRO. Dotted curve, depleted output pump pulse. Dashed curve, signal + idler output pulse. The upturn of the reflected pump pulse at the middle of the trace indicates that the DRO is driven beyond the point of maximum depletion.

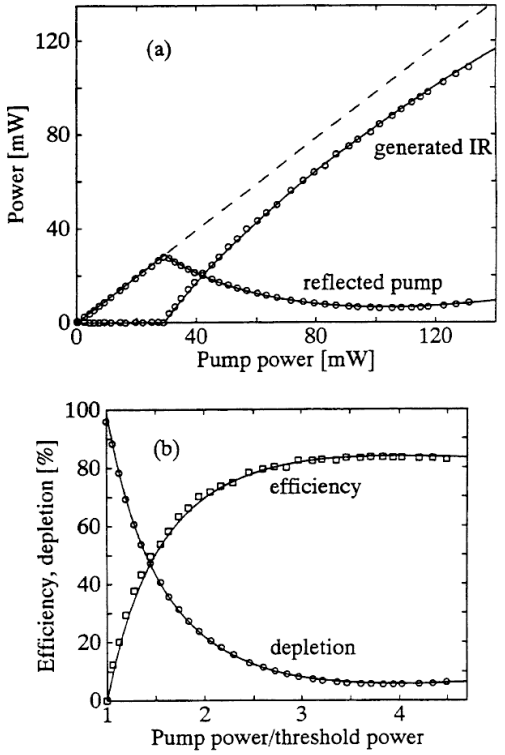

Fig. 3. (a) Output pump and combined signal and idler power as a function of pump power, (b) conversion efficiency and depletion as a function of normalized pump power. Maximum conversion efficiency of 84% and maximum pump depletion (95%) are reached at four times above threshold. The data are from Fig. 2. The solid curves are theoretical fits explained in the text.

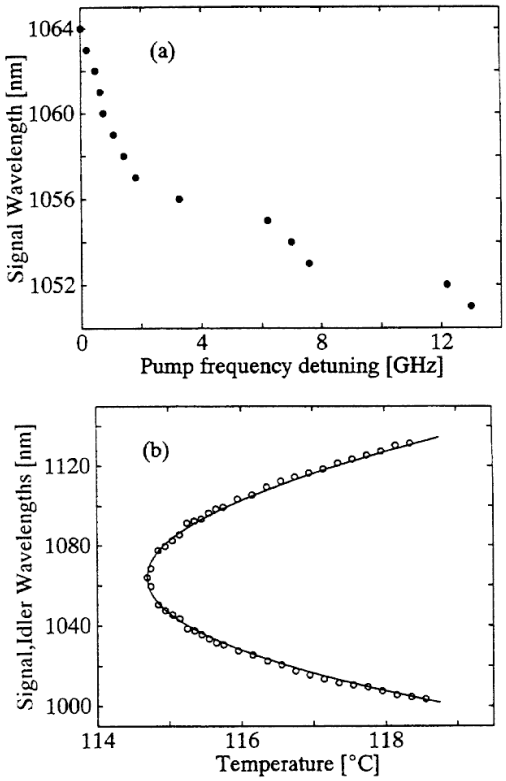

Fig. 4. Output wavelengths of the DRO as a function of (a) the pump frequency, (b) the crystal temperature.

ation of the signal and the idler frequencies from the cavity frequencies. By locking the pump frequency to zero out the error signal, the sum of signal and idler detuning is kept to zero, which is equivalent to fulfillment of the cluster condition. The servo system acts on the fast frequency control of the laser, which consists of a piezoelectric ceramic bonded to the laser cavity. Because a tuning range of approximately ± 50 MHz is accessible, Eq. (24) indicates that temperature changes of as much as ± 10 mK or length changes of as much as ± 1.4 nm can be followed with the present servo system.

In the present experiment, with the laser frequency stabilized to the DRO, mode-hop-free, single-frequency signal and idler output was typically maintained for more than 10 min. Over a period of 1 h occasional mode hops occurred. Without stabilization, mode hops typically occurred every few tens of seconds. The mode hops may be due to sporadic fluctuations in the length or the temperature of the cavity that exceed the capabilities of the servo system. A combined signal and idler power of 105 mW was generated under lock, at a conversion efficiency of 81%. This conversion efficiency was slightly reduced compared with operation in the long-pulse mode as a result of slight changes in the mode-matching efficiency $1 - \epsilon$ caused by thermal effects in the resonator.

Coarse tuning of DRO output by pump frequency variation is shown in Fig. 4(a). By variation of the laser frequency over 6 GHz at a fixed temperature close to the degeneracy point, the signal and the idler wavelengths could each be tuned over more than 10 nm. In this measurement the crystal temperature and length are not changed, so that the tuning contains both mode and cluster hops. In the absence of these effects the range of tuning predicted by Eq. (19) is ± 7.3 nm.

Temperature tuning of the DRO at fixed pump frequency covered the range from 1004 to 1132 nm limited by the bandwidth of the dielectric mirrors [Fig. 4(b)]. The curve is the $\Delta k = 0$ curve according to Eq. (19), with a fitted reference temperature.

4. CONCLUSION

In this paper we have presented a theoretical and experimental study of the conversion efficiency and the depletion of a doubly optical parametric oscillator (DRO). We found excellent agreement between a general treatment of focused wave interactions in the presence of phase mismatch and the experimental data obtained with a cavity exhibiting strongly focused modes. It has been shown that the maximum conversion efficiency is always reached at four times above threshold and is equal to the escape efficiency of the cavity, independent of wave-vector mismatch, provided that signal and idler modes oscillate with zero net detuning. This condition arises from the occurrence of nonlinear detunings above threshold under phase-mismatched conditions.

We have also demonstrated an actively frequency-stabilized cw DRO that operated over significant periods of time with single-frequency output and a visible-to-infrared power conversion of 81%, to our knowledge the highest demonstrated so far. The unoptimized infrared-to-infrared conversion efficiency was 35%. Tens of minutes of mode-hop-free operation through active stabilization represents an improvement from the previous state of the art.[22,23] The high stability and efficiency demonstrated represent an important step toward a practical use of DRO's. With regard to future developments, the externally resonantly doubled monolithic Nd:YAG laser, with its 20-GHz continuous tuning range at 532 nm, is well suited for applications in which a significant continuous tuning range of DRO output is desired.

The operating regime several times above threshold explored in this study is also of interest for quantum optical studies. It offers the possibility of verifying a number of theoretical predictions, one of which is a substantial reduction in the quantum fluctuations of the phase quadrature of the depleted harmonic wave.[24] The high conversion efficiency achievable in above-threshold operation also implies that the resonator is suitable for the generation of squeezed vacuum below threshold[25] and of strongly intensity-correlated twin beams.[26]

ACKNOWLEDGMENTS

We are very grateful to R. Paschotta for his participation in developing the frequency doubler, to R. Bruckmeier and A. G. White for important discussions, and to S. F. Pereira for her assistance. This research was supported by the Deutsche Forschungsgemeinschaft, the European Community Basic Research Project 6934 QUINTEC, and the European Community Human Capital and Mobility Network "Non-classical Light."

S. Schiller's e-mail address is schiller@uni-Ronstanz.de.

Note added in proof: After submission of this paper, a publication appeared describing single-frequency operation of a type-II KTP DRO. Operation without mode hops for periods of time similar to those observed here was achieved through active stabilization.[27]

REFERENCES AND NOTES

1. Z. Y. Ou, S. F. Pereira, E. S. Polzik, and H. J. Kimble, "85% Efficiency for cw frequency doubling from 1.08 to 0.54 μm," Opt. Lett. **17,** 640–642 (1992).
2. R. Paschotta, K. Fiedler, P. Kürz, R. Henking, S. Schiller, and J. Mynlek, "82% Efficient continuous-wave frequency doubling of 1.06 μm with a monolithic MgO:$LiNbO_3$ resonator," Opt. Lett. **19,** 1325–1327 (1994); erratum, Opt. Lett. **20,** 345 (1995).
3. E. S. Polzik, J. Carri, and H. J. Kimble, "Atomic spectroscopy with squeezed light for sensitivity beyond the vacuum-state limit," Appl. Phys. **55,** 279–290 (1992).
4. A. E. Siegman, "Nonlinear optical effects: an optical power limiter," Appl. Opt. **1,** 739–744 (1962).
5. J. E. Bjorkholm, "Analysis of the doubly resonant optical parametric oscillator without power-dependent reflections," IEEE J. Quantum Electron. **QE-5,** 293–295 (1969); J. E. Bjorkholm, A. Ashkin, and R. G. Smith, "Improvement of optical parametric oscillators by nonresonant pump reflection," IEEE J. Quantum Electron. **QE-6,** 797–799 (1970).
6. C. D. Nabors, R. C. Eckardt, W. J. Kozlovsky, and R. L. Byer, "Efficient, single-axial-mode operation of a monolithic MgO:$LiNbO_3$ optical parametric oscillator," Opt. Lett. **14,** 1134–1136 (1989).
7. R. Bruckmeier, A. G. White, S. Schiller, and J. Mlynek, Fakultät für Physik, Universität Konstanz, D-78434 Konstanz, Germany (personal communication, 1995).
8. A. Yariv and P. Yeh, *Optical Waves in Crystals* (Wiley, New York, 1984), Chap. 12.5.
9. L.-A. Wu and H. J. Kimble, "Interference effects in second-harmonic generation within an optical cavity," J. Opt. Soc. Am. B **2,** 697–703 (1985).
10. T. Debuisschert, A. Sizmann, E. Giacobino, and C. Fabre, "Type-II continuous-wave optical parametric oscillators: oscillation and frequency-tuning characteristics," J. Opt. Soc. Am. B **10,** 1668–1680 (1993).
11. W. Brunner, H. Paul, and A. Bandilla, "Fluktuationen beim optischen parametrischen Oszillator," Ann. Phys. (Leipzig) **27,** 82–90 (1971).
12. L. A. Lugiato, C. Oldano, C. Fabre, E. Giacobino, and R. J. Horowicz, "Bistability, self-pulsing and chaos in optical parametric oscillators," Nuovo Cimento D **10,** 959–977 (1988).
13. R. Paschotta, M. J. Collett, P. Kürz, K. Fiedler, H.-A. Bachor, and J. Mlynek, "Bright squeezed light from a singly resonant frequency doubler," Phys. Rev. Lett. **72,** 3807–3810 (1994).
14. S. Schiller, S. Kohler, R. Paschotta, and J. Mlynek, "Squeezing and quantum nondemolition measurements with an optical parametric amplifier," Appl. Phys. B. **60,** S77–S88 (1995).
15. S. Schiller, G. Breitenbach, S. F. Pereira, R. Paschotta, A. G. White, and J. Mlynek, "Generation of continuous-wave bright squeezed light," in *Laser Frequency Stabilization and Noise Reduction,* Y. Shevy, ed., Proc. Soc. Photo-Opt. Instrum. Eng. **2378,** 91–98 (1995). The phase-matching coefficient K, denoted by B in this reference, can have an arbitrary phase.
16. G. D. Boyd and D. A. Kleinman, "Parametric interaction of focussed Gaussian light beams," J. Appl. Phys. **39,** 3597–3639 (1968).
17. R. C. Eckardt, C. D. Nabors, W. J. Kozlovsky, and R. L. Byer, "Optical parametric oscillator frequency tuning and control," J. Opt. Soc. Am. B **8,** 646–676 (1991). In Eq. (A1), read $A_3 + B_2F$ instead of $A_3 - B_2F$.
18. S. Schiller and R. L. Byer, "Quadruply resonant optical parametric oscillation in a monolithic total-internal-reflection resonator," J. Opt. Soc. Am. B **10,** 1696–707 (1993).
19. W. J. Kozlovsky, C. D. Nabors, R C. Eckardt, and R. L. Byer, "Monolithic MgO:$LiNbO_3$ doubly resonant optical parametric oscillator pumped by a frequency-doubled diode-laser-pumped Nd:YAG laser," Opt. Lett. **14,** 66–68 (1989).
20. D. C. Gerstenberger and R. W. Wallace, "Continuous-wave operation of a doubly resonant lithium niobate optical parametric oscillator system tunable from 966 to 1185 nm," J. Opt. Soc. Am. B **10,** 1681–1683 (1993).
21. R. Drever, J. Hall, F. Kowalski, J. Hough, G. Ford, A. Munley, and H. Ward, "Laser phase and frequency stabilization using an optical resonator," Appl. Phys. B **31,** 97 (1983).
22. D. Lee and N. C. Wong, "Stabilization and tuning of a doubly resonant optical parametric oscillator," J. Opt. Soc. Am. B **10,** 1659–1667 (1993).
23. F. G. Colville, M. J. Padgett, and D. H. Dunn, "Continuous-wave, dual-cavity, doubly resonant, optical parametric oscillator," Appl. Phys. Lett. **64,** 1490–1492 (1994).
24. M. J. Collett and D. F. Walls, "Squeezing spectra for nonlinear optical systems," Phys. Rev. A **32,** 2887–2892 (1985).
25. G. Breitenbach, T. Müller, S. F. Pereira, J.-Ph. Poizat, S. Schiller, and J. Mlynek, "Squeezed vacuum from a monolithic optical parametric oscillator," J. Opt. Soc. Am. B **12,** 2304–2309 (1995).
26. C. D. Nabors and R. M. Shelby, "Two-color squeezing and sub-shot-noise signal recovery in doubly resonant optical parametric amplifier," Phys. Rev. A **42,** 556–559 (1990).
27. A. J. Henderson, M. J. Padgett, J. Zhang, W. Sibbett, and M. H. Dunn, "Continuous frequency tuning of a cw optical parametric oscillator through tuning of its pump source," Opt. Lett. **20,** 1029–1031 (1995).